

Supporting Information

Controlled flexibility of porous coordination polymers by shifting the position of -CH₃ group around coordination sites and their high efficient gas separation

Jingui Duan,^{*,a} Qiang Zhang,^a Suna Wang,^b Bihang Zhou,^a Jiajia Sun,^a Wanqin Jin^a

^a State Key Laboratory of Materials-Oriented Chemical Engineering, College of Chemical
Engineering, Nanjing Tech University, Nanjing 210009, China
Email: duanjingui@njtech.edu.cn

^b School of Chemistry and Chemical Engineering, Liaocheng University, Liaocheng, 252059,
China

Materials and methods

All air-sensitive reactions were carried out under dry N₂ using standard Schlenk techniques. All the reagents and solvents were commercially available and used as received. The FTIR spectra were recorded in the range of 4000-600 cm⁻¹ on a Nicolet ID5 ATR spectrometer. Thermal analyses (TG) were performed on a Universal V3.9A TA Instruments from room temperature to 700°C with a heating rate of 10°C/min under flowing nitrogen. The powder X-ray diffraction patterns (PXRD) measurements were carried on a Bruker AXS D8 Advance 40kV, 40mA for CuKα (θ= 1.5418 Å) with a scan rate of 0.2 s/deg at room temperature. Simulated powder patterns from single-crystal X-ray diffraction data were generated using Mercury 1.4.2 software.

Adsorption Experiments

Before measurement, solvent-exchanged samples were prepared by immersing the as-synthesized crystals in dehydrated methanol for two days to remove the nonvolatile solvents, and the extract was decanted every 8h and fresh methanol was replaced. The completely activated sample was obtained by heating the solvent-exchanged sample at room temperature for 4h, 60°C for 4h and then 120°C for 24h under a dynamic high vacuum. In the gas sorption measurements, ultra-high-purity grade gases were used throughout the adsorption experiments. Gas adsorption isotherms were obtained using a Belsorp volumetric adsorption instrument from BEL Japan.

Estimation of the isosteric heats of gas adsorption

A Virial-type expression comprising the temperature-independent parameters a_i and b_i was employed to calculate the enthalpies of adsorption for CO₂ (at 273, 283 and 298K) on NTU-40 and NTU-41. In each case, the data were fitted using the equation:

$$\ln P = \ln N + 1/T \sum_{i=0}^m a_i N^i + \sum_{i=0}^n b_i N^i \quad (1)$$

Here, P is the pressure expressed in Torr, N is the amount adsorbed in mmol/g, T is the temperature in K, a_i and b_i are virial coefficients, and m , n represent the number of coefficients required to adequately describe the isotherms (m and n were gradually increased until the contribution of extra added a and b coefficients was deemed to be statistically insignificant towards the overall fit, and the average value of the squared deviations from the experimental values was minimized).

$$Q_{st} = -R \sum_{i=0}^m a_i N^i \quad (2)$$

Here, Q_{st} is the coverage-dependent isosteric heat of adsorption and R is the universal gas constant.

From these results, the Henry's constant (K_H) is calculated from where T is temperature.

$$K_H = \exp(-b_0) \exp(-a_0 / T) \quad (3)$$

The Henry's Law selectivity for gas component i over j at 273 and 298 K were calculated based on Eq. 4.

$$S_{ij} = K_{Hi}/K_{Hj} \quad (4)$$

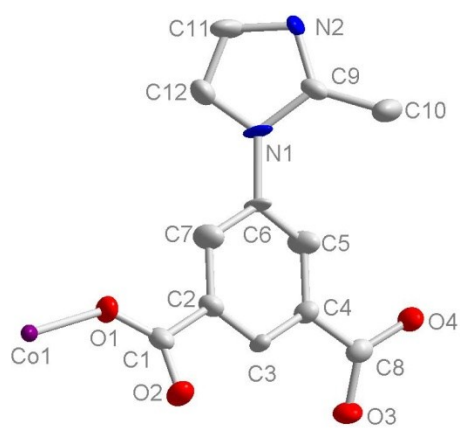


Figure S1 View of the asymmetric unit of NTU-40.

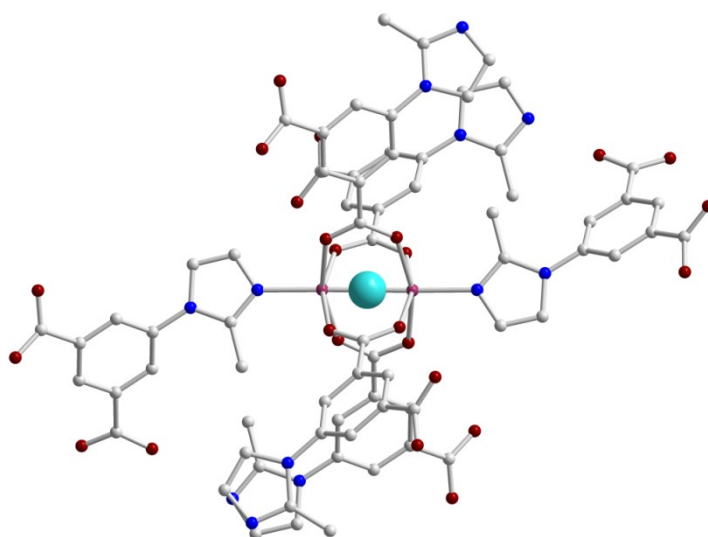


Figure S2 View of the cluster connection of NTU-40.

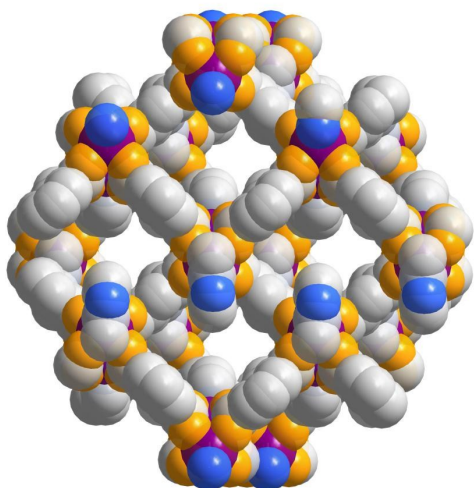


Figure S3 View of the crystal packing and its window aperture along a-axis in NTU-40.

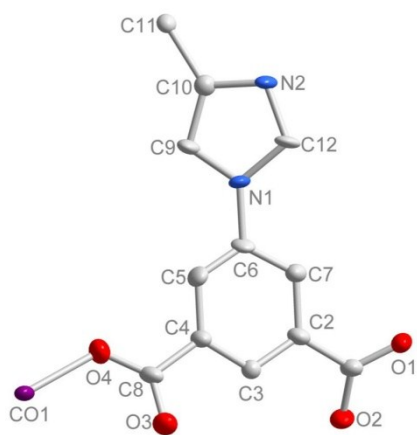


Figure S4 View of the asymmetric unit of NTU-41.

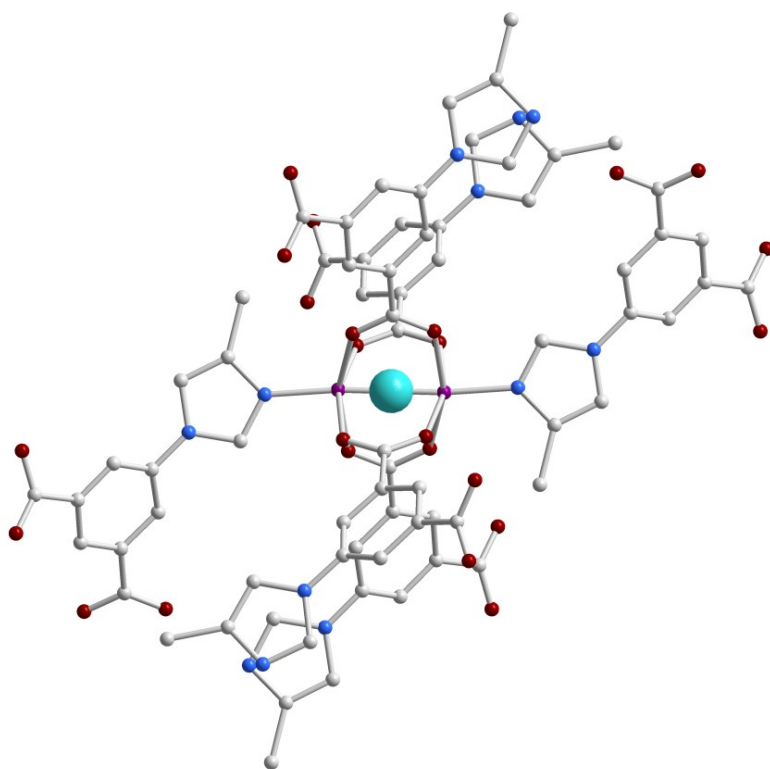


Figure S5 View of the cluster connection of NTU-41.

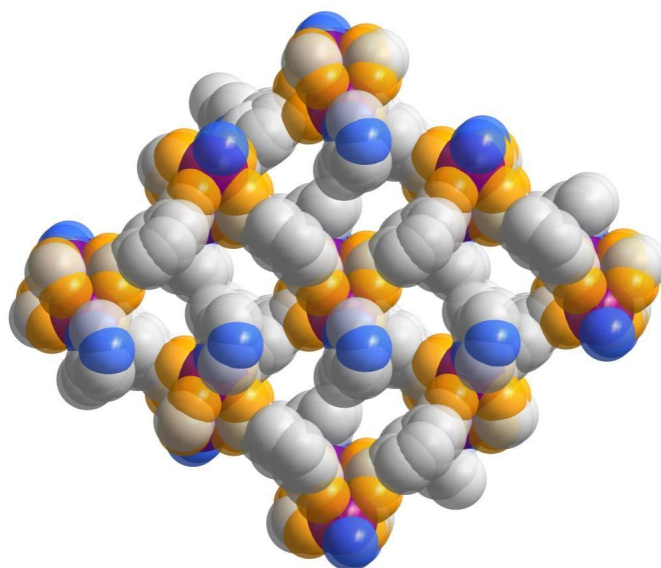


Figure S6 View of the crystal packing and tailored pore size along a-axis in NTU-41.

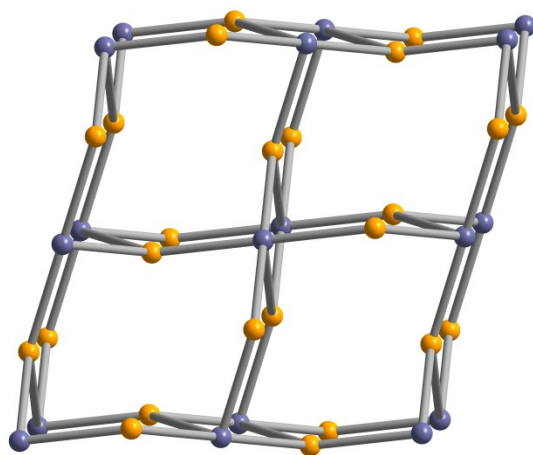
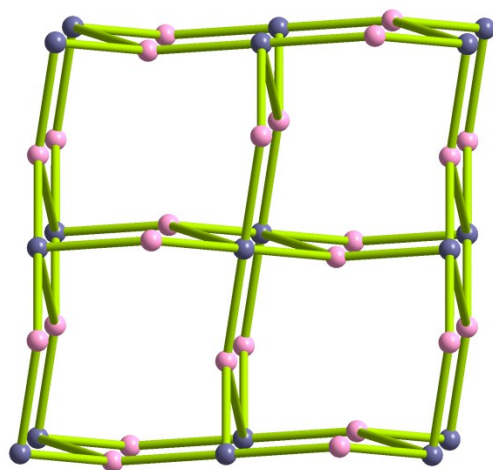


Figure S7 View of the **apo** topology in NTU-40 (up) and NTU-41 (down).

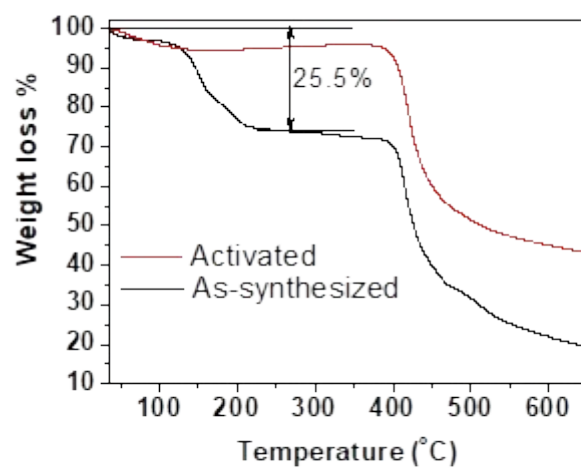


Figure S8 TG analysis of NTU-40 and its activated phase.

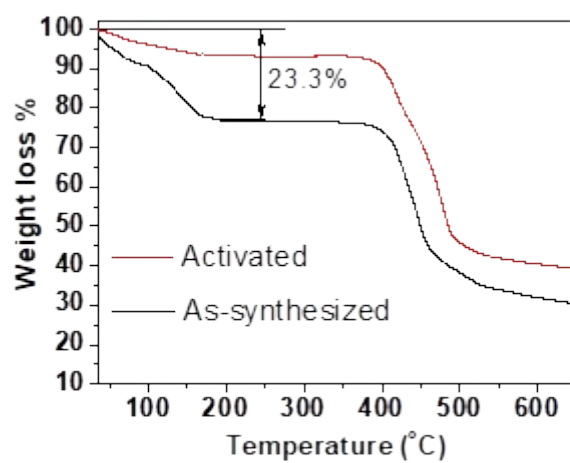


Figure S9 TG analysis of NTU-41 and its activated phase.

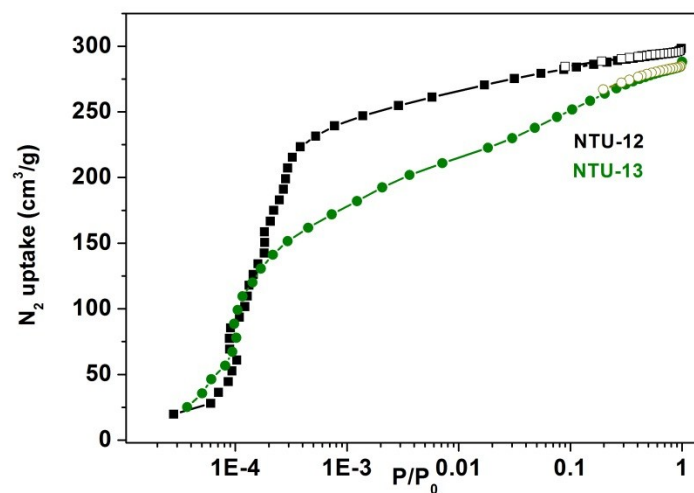


Figure S10 N_2 adsorption isotherms (at 77K) of NTU-12 and NTU-13 (reported by us in J. Mat. Chem. A, 2017, 5, 17874).

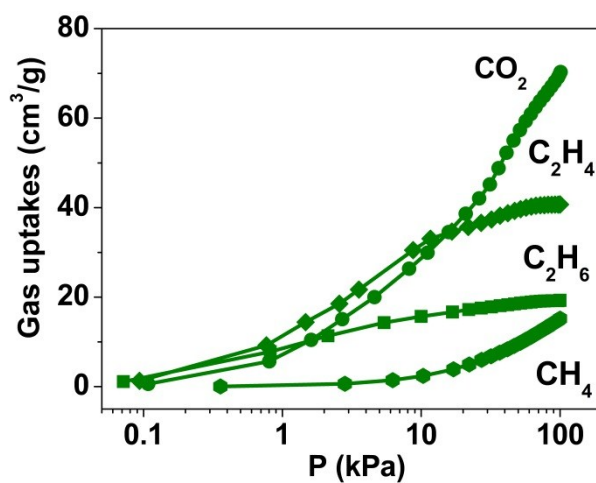


Figure S11 View of the adsorption isotherms of NTU-40 at 273 K (Log scale of pressure).

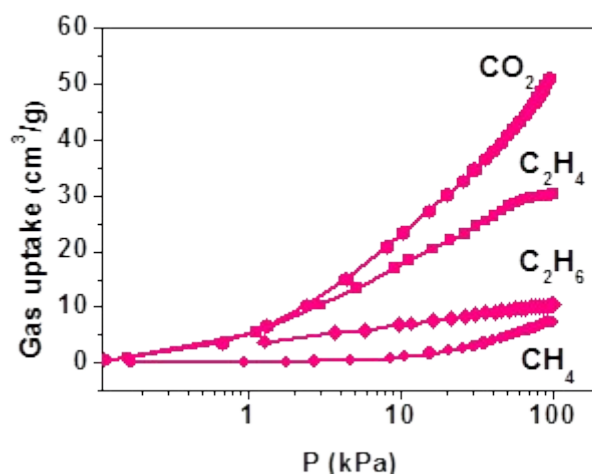


Figure S12 View of the adsorption isotherms of NTU-41 at 273 K (Log scale of pressure).

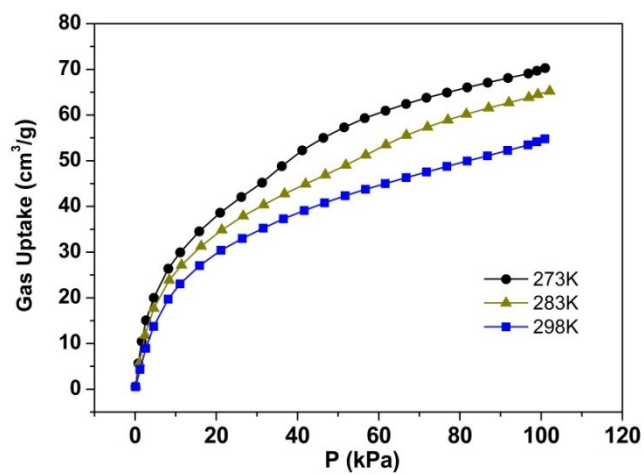


Figure S13 CO₂ gas uptakes of NTU-40.

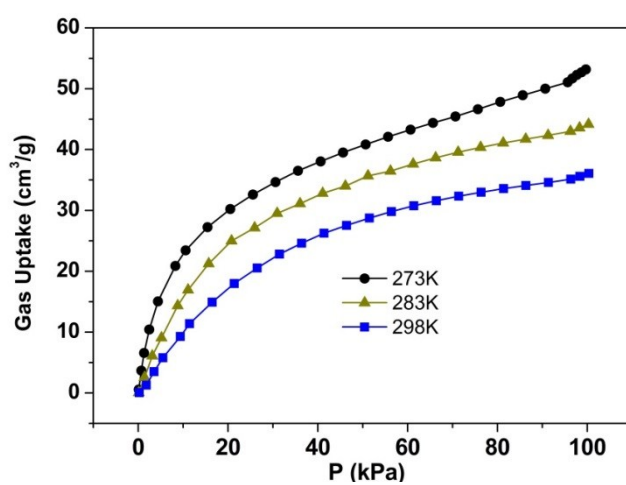


Figure S14 CO₂ gas uptakes of NTU-41.

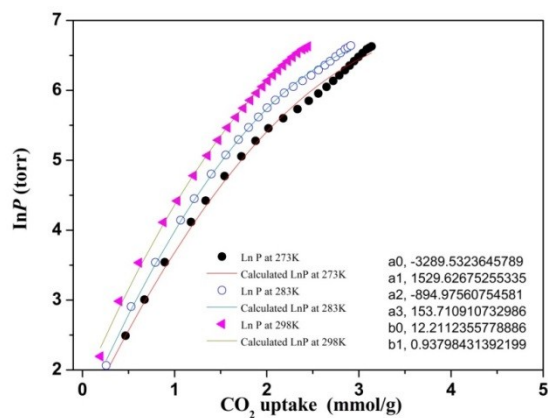


Figure S15 The calculated virial equation isotherms parameters fit to the experimental CO₂ data of NTU-40.

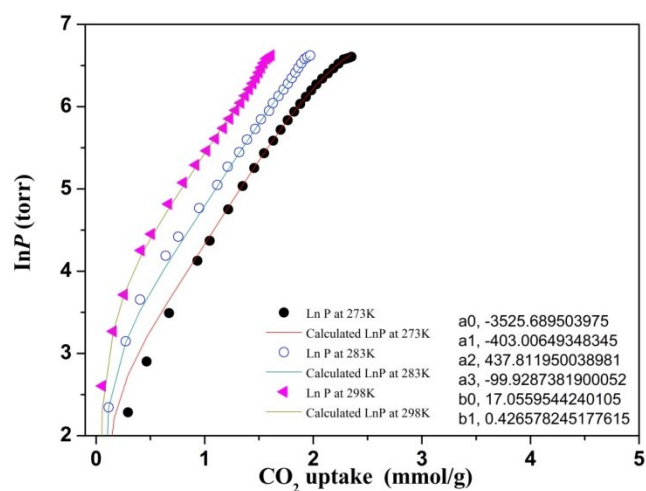


Figure S16 The calculated virial equation isotherms parameters fit to the experimental CO₂ data of NTU-41.

Table S1 Parameters of isotherm fitting for NTU-40 and NTU-41.

For NTU-40				
	CH ₄	C ₂ H ₄	C ₂ H ₆	CO ₂
a1	0.013520174	0.040022637	0.736536	1.973159786
a2	1.630344926	1.852688947	0.15195	1.579166555
b1	6.10E-09	5.82E-20	1.068687	7.53E-04
b2	0.006626639	0.350248378	0.006463	0.243503482
c1	6.46152638	11.89911965	0.987291	1.857866617
c2	1.00684931	0.942984021	1.51028	1.079099134
For NTU-41				
	CH ₄	C ₂ H ₄	C ₂ H ₆	CO ₂
a1	0.447531356	0.384236	0.736536	1.180089
a2	0.05031814	0.172392	0.15195	2.963917
b1	0.009307802	0.092148	1.068687	2.05E-01
b2	1.98E-09	2.55E+00	0.006463	0.010474
c1	1.133636748	0.770608	0.987291	1.011929
c2	5.151537686	1.241751	1.51028	0.883057

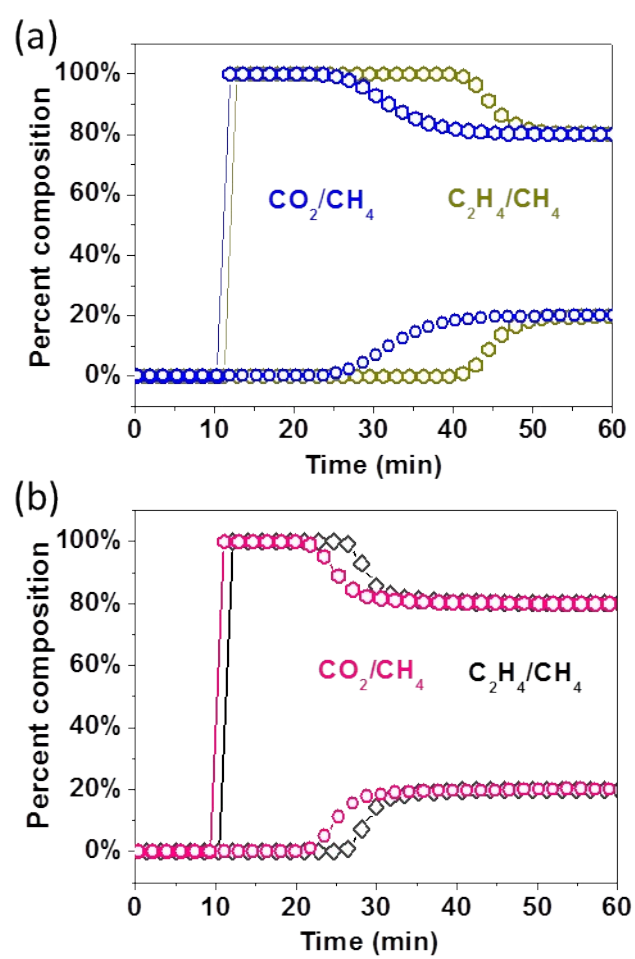


Fig. S17 Normalized breakthrough curves (1g) of NTU-40 (a) and NTU-41 (b) from 300mg and 280mg, respectively.